dizing equivalents. Reductive damage at C leads to an enhanced probability of deposition of oxidative damage at G, and oxidation of G sensitizes C to become an even better trap for electrons.[51]

A final comment may be made on the observation[4a-e] that in DNA irradiated at or warmed up to room temperature the negative charge created on ionization ultimately ends up as the "C6-protonated thymine radical anion", the 5,6-dihydrothymine-5-yl radical T(H)•, or more precisely, T(C6H)•. This

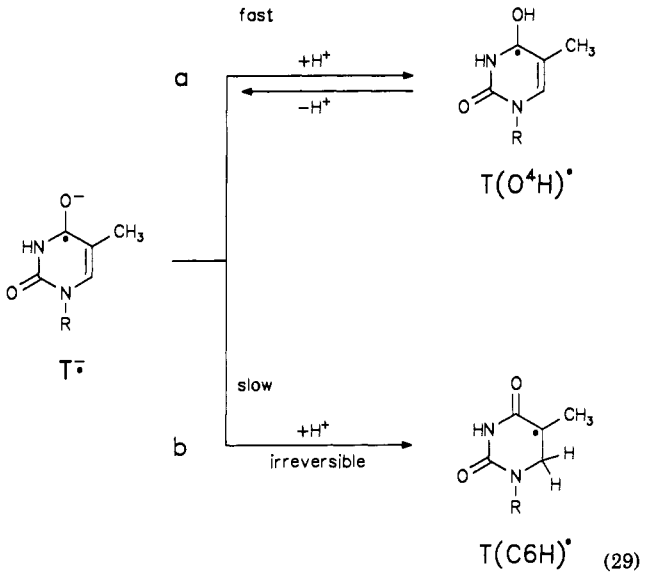

(29)

is the result of the irreversibility[20,21] of this protonation on carbon. In the case of cytidine, there is so far no evidence for an analogous reaction in aqueous solution.[12c,54] Since the N3 (or the tautomeric O^2) protonated electron adduct of cytidine is able to donate an electron in aqueous solution,[24,55] even to weak electron acceptors such as 1,4-DMP$^+$ (see Table I) or to orotic acid[45] (see Table II), it is conceivable that it is able in DNA to transfer an e^- to thymidine, where it will be finally trapped by protonation of C6 (eq 29b).[56] In other words, although in DNA an electron has a better chance of being at first trapped at C, due to the strong driving force for protonation of the electron adduct, the *final* site of deposition, the "burial site", will be T, where it is trapped, after transfer along the helix axis, by the irreversible protonation of carbon. This explains the firmly established[3,4,15] formation of T(H)• in DNA irradiated at or warmed up to room temperature.

Acknowledgment. The financial support from a travel grant (Nato 0748/85) is gratefully acknowledged. J. P. Telo and L. P. Candeias thank the Deutscher Akademischer Austauschdienst (DAAD) for stipends.

Registry No. Uracil, 66-22-8; uridine, 58-96-8; deoxyuridine, 951-78-0; uridine-3′-phosphate, 84-53-7; uridine-5′-phosphate, 58-97-9; uridine-3′,5′-diphosphate, 2922-95-4; thymine, 65-71-4; thymidine, 50-89-5; thymidine-3′-phosphate, 2642-43-5; thymidine-5′-phosphate, 365-07-1; 6-methyluracil, 626-48-2; orotic acid, 65-86-1; isoorotic acid, 23945-44-0; cytosine, 71-30-7; cytidine, 65-46-3; cytidine-5′-phosphate, 63-37-6.

(54) However, on irradiation of cytosine in the solid state at 300 K, H-addition to C5 and C6 has been observed (Flossmann, W.; Westhof, E.; Müller, A. *Int. J. Radiat. Biol.* **1976**, *30*, 301).

(55) Greenstock, C. L.; Dunlop, I. *Radiat. Res.* **1973**, *56*, 428.

(56) In DNA, the C5–C6 double bond of T is exposed to the outside of the helix. In this region, water molecules (~6 per base pair, located mainly in the minor groove) are available to protonate C6. This reaction requires the presence of negative charge at C6. It is likely that protonation of O^4, which leads to a decrease of charge density also at C6, would decrease the rate of C6 protonation considerably, see ref 20), and thereby protect T. However, due to the low acidity of adenine, $T^{\bullet-}$ remains an anion and can thus be irreversibly protonated by water at C6.

Nickel(II) Ion–Support Interactions as a Function of Preparation Method of Silica-Supported Nickel Materials

Olivier Clause,*,† Maggy Kermarec,‡ Laurent Bonneviot,‡,§ Françoise Villain,‡,∥ and Michel Che‡

Contribution from the Laboratoire de Réactivité de Surface et Structure, URA 1106 CNRS, Université Pierre et Marie Curie, 4 place Jussieu, 75252 Paris Cedex 05, France, and Institut Français du Pétrole, BP 311, 92506 Rueil-Malmaison Cedex, France. *Received May 8, 1991*

Abstract: The adsorption on silica of various amminenickel(II) complexes has been investigated as a function of the preparation procedure, i.e., the composition of the impregnating solution and the washing and drying steps. Quite different adsorption modes can be distinguished by EXAFS, XANES, and infrared spectroscopies depending on the pH of the impregnating solution: $[Ni(NH_3)_6]^{2+}$ weakly adsorbs (electrostatic adsorption) while $[Ni(H_2O)_{6-n}(NH_3)_n]^{2+}$ ($n < 6$) complexes strongly interact with the carrier, giving rise to the formation of layered nickel silicate structures. A classification of the bonding of cations on supports, the latter acting as dispersing agents, macroanions, or chemical reagents, is proposed. The EXAFS technique is shown to be a powerful tool for the determination of the ion–support interaction during the first steps of the preparation of silica-supported nickel materials.

Studies focusing on ion adsorption on clays, inorganic oxides, and colloids have received much attention in a variety of domains, such as catalysis,[1-4] clay chemistry,[5] electrochemistry at the oxide/electrolyte interface,[6-11] and materials science.[12-14]

The present paper concerns silica-supported nickel materials prepared by deposition from aqueous solutions. Nickel supported

* To whom correspondence should be addressed.
† Institut Français du Pétrole.
‡ Université Pierre et Marie Curie.
§ Present address: Département de Chimie, Université Laval, G1V1E6, Québec, Canada.
∥ Present address: LURE, Université Paris-Sud, 91405 Orsay, France.

(1) See, for instance: Hegedus, L. L.; Avis, R.; Bell, A. T.; Boudart, M.; Chen, N. Y.; Gates, B. T.; Haag, W. O.; Somorjai, G. A.; Wei, J. *Catalyst Design, Progress and Perspectives*; Wiley: New York, 1987.

(2) Che, M.; Bennett, C. O. *Adv. Catal.* **1989**, *36*, 55–172.

(3) Che, M.; Bonneviot, L. *Successful Design of Catalysts*; Elsevier: Amsterdam, 1988; pp 147–158.

(4) Marcilly, C.; Franck, J. P. *Rev. Inst. Fr. Pet.* **1984**, *3*, 337–364.

(5) See, for instance: Barrer, R. M. *Zeolites and Clay Minerals as Sorbents and Molecular Sieves*; Academic Press: London, 1978.

0002-7863/92/1514-4709$03.00/0

on alumina, silica, or silica–alumina materials has found widespread application in hydrogenation and hydrogenolysis processes, such as the steam-reforming of methane and higher paraffins or the methanation of coal synthesis gas.[15] Alumina-supported nickel materials are usually synthesized from hydrotalcite-type precursors by coprecipitation from Ni(II) and Al(III) salts,[16-18] whereas silica-supported nickel materials are most commonly prepared by incipient wetness impregnation, ion-exchange, and deposition–precipitation techniques.[19,20] It is well recognized that Ni/SiO_2 precursors produced by these various methods exhibit very different characteristics in the calcined and the reduced states. For example, high reduction temperatures are required if the precursors are prepared by ion-exchange or deposition–precipitation methods, whereas temperatures lower than 400 °C are generally sufficient when the precursors are prepared by incipient wetness impregnation.[21,22] The activation procedure, i.e., the calcination temperature and the reducing gas composition, is of major importance. However, the nature of the ion–support interaction in the precursor has a strong influence on the size distribution and the thermal stability of the metal oxide particles in the calcined state. The importance of the initial steps of the preparation is hence emphasized. A better understanding of the nature of the interactions between the transition-metal ions and the carrier at the solid–liquid interface is clearly needed.

The various roles played by silica in the impregnation of Ni/SiO_2, Cu/SiO_2, and Zn/SiO_2 catalysts with aqueous metal ammine and ethylenediamine solutions have been previously studied.[23,24] From these studies, a classification of the strength of different ion–support interactions was proposed.[25] The following ion–support interactions may be distinguished: the recrystallization of the precursor in the porosity of the silica, the latter acting as a microporous container; an electrostatic adsorption of cations, where the support becomes a counteranion without modification of the inner sphere of coordination; the grafting of isolated ions onto the support, which plays the role of a mono- or bidentate macroligand; the formation of silicates from silica, which acts as a reactant.

A previous EXAFS study showed that the deposition–precipitation of Ni(II) ions onto silica gives rise to the formation of nickel silicates with layer structure. $Ni(OH)_2$ was not observed (i.e., neither trapped in the porosity nor "glued" onto silicate layers) in the washed samples. Thus silica was found to act as a reactant.[26]

In this work, the role of silica is investigated during impregnation by ammonia solutions of various Ni(II) concentrations, at different pH with or without subsequent washing operations. Silica-supported nickel materials prepared by ion exchange, with Ni(II) ammonia solutions, have been extensively studied in the past 20 years. However, the nature of the adsorbed Ni(II) species is not clear: exchanged $[Ni(NH_3)_6]^{2+}$,[27] grafted $[Ni(NH_3)_4]^{2+}$ onto the silica surface,[28-30] and silicate formation have been suggested.[20,31,32] In the latter case, it is not clear whether the formation of silicates occurs during impregnation or calcination. The washing step has also recently been shown to play an important role.[30] The differences in interpretation, of the interaction between Ni(II) ammonia solutions and silica, are most likely due to the necessity to use characterization techniques that are not well adapted for the various stages of catalyst preparation, in particular for ion-exchange silica gels, which are very difficult to characterize. Thermal analysis techniques induce structural modifications and are thus excluded. Undried impregnated silicas are generally X-ray amorphous. UV diffuse reflectance spectroscopy can only bring information on the local symmetry around the adsorbed ions. EXAFS and XANES spectroscopies, by contrast, have been shown to be powerful tools for studying X-ray amorphous impregnated precursors, enabling the determination of the exact nature of adsorbed species.[25] A detailed description of the various roles played by the support during impregnation, washing, and drying is presented in this paper. IR spectroscopy has also been used, as a complementary technique, to provide evidence for nickel silicate formation in the 600–750-cm^{-1} region in freshly prepared samples.

Experimental Section

Samples Prepared by Ion Exchange. Ni/SiO_2 precursors were prepared by cation exchange from 70 mL of 0.01, 0.05, or 0.1 M nickel nitrate solutions containing 1 M ammonium nitrate on 5 g of spherosil XOA 400 silica (provided by Rhône-Poulenc; specific surface area, 400 $m^2 g^{-1}$; mean pore diameter, 8 nm). The pH was adjusted to the desired value ($5 < pH < 11$) by bubbling gaseous NH_3 in the exchange solutions before adding silica. The suspensions were kept at 298 K in a thermostated vessel and stirred during 24 h to reach the thermodynamic equilibrium of adsorption. The exchange solutions were then filtered, their pH was measured, and the final nickel(II) concentrations were determined by an EDTA titration method using murexid as the colored indicator. The amounts of Ni(II) adsorbed onto silica at thermodynamic equilibrium were derived from the difference of Ni(II) concentrations in the exchange solutions before and after exchange. The silica gels were washed with aqueous solutions containing 1 M ammonium nitrate and with the same pH as those of the impregnating solutions at equilibrium. The impregnated samples were then dried overnight at 120 °C in an oven.

Samples Prepared by Incipient Wetness Impregnation. Two sets of Ni/SiO_2 precursors with 1.4 and 3.5 wt % Ni were prepared by incipient wetness impregnation of SiO_2 with 0.2 and 0.5 M, respectively, solutions of nickel nitrate containing 1 M of ammonium nitrate, the pH being adjusted by bubbling NH_3 gas. The impregnated samples were then dried overnight at 120 °C in an oven.

In what follows, the precursors are referred to as x%E(I)y, where E and I stand for ion-exchange and incipient wetness impregnation, respectively, and x% and y correspond to the Ni loading and the pH of the impregnating solution, respectively.

EXAFS and XANES Measurements. EXAFS measurements were performed at the LURE radiation synchrotron facility by using the X-ray beam emitted by the DCI storage ring (positron energy 1.85 GeV; ring

(6) Adamson, A. W. *Physical Chemistry of Surfaces*; Wiley: New York, 1982; pp 185–231.
(7) Lyklema, J. *J. Electroanal. Chem.* **1968**, *18*, 341–348.
(8) Healy, T. W.; White, L. R. *Adv. Colloid Interface Sci.* **1978**, *9*, 303–345.
(9) Davis, J. A.; James, R. O.; Leckie, J. O. *J. Colloid Interface Sci.* **1978**, *63*, 480–499.
(10) Sprycha, R. *J. Colloid Interface Sci.* **1984**, *102*, 173–185.
(11) Van Riemsdijk, W. H.; De Wit, J. C. M.; Koopal, L. K.; Bolt, G. H. *J. Colloid Interface Sci.* **1987**, *116*, 511–522.
(12) See, for instance: *Adsorption from Solution*; Ottewill, R. H., Rochester, C. H., Smith, A. L., Eds.; Academic Press: London, 1983.
(13) James, R. O.; Davis, J. A.; Leckie, J. O. *J. Colloid Interface Sci.* **1978**, *65*, 331–344.
(14) Van Riemsdijk, W. H.; Bolt, G. H.; Koopal, L. K.; Blaakmeer, J. *J. Colloid Interface Sci.* **1986**, *109*, 219–228.
(15) Satterfield, C. N. *Heterogeneous Catalysis in Practice*; Mac Graw-Hill: New York, 1980. Bond, G. C. *Heterogeneous Catalysis*; Oxford University Press: Oxford, 1988.
(16) Puxley, D. C.; Kitchener, I. J.; Komodromos, C.; Parkyns, N. D. *Preparation of Catalysts III*; Elsevier: Amsterdam, 1983; pp 237–269.
(17) Kruissink, E. C.; Van Reijen, L. L.; Ross, J. R. H. *J. Chem. Soc., Faraday Trans. 1* **1981**, *77*, 649–663.
(18) Clause, O.; Rebours, B.; Merlen, E.; Trifiro', F.; Vaccari, A. *J. Catal.* **1992**, *133*, 231–246.
(19) Houalla, M.; Delannay, F.; Matsuura, I.; Delmon, B. J. *Chem. Soc., Faraday Trans 1* **1980**, *76*, 2128–2141.
(20) Coenen, J. W. E. In *Preparation of Catalysts II*, Poncelet, G., Ed.; Elsevier: Amsterdam, 1979; pp 89–111.
(21) Montes, M.; Soupart, J. B.; De Saedeleer, M.; Hodnett, B. K.; Delmon, B. *J. Chem. Soc., Faraday Trans 1* **1984**, *80*, 3209–3220.
(22) Tohji, K.; Udagawa, Y.; Tanabe, S.; Ueno, A. *J. Am. Chem. Soc.* **1984**, *106*, 612–617.
(23) Clause, O.; Bonneviot, L.; Che, M.; Verdaguer, M.; Villain, F.; Bazin, D.; Dexpert, H. *J. Chim. Phys.* **1989**, *86*, 1767–1775. Che, M.; Clause, O.; Bonneviot, L. *Proc. 9th Int. Congr. Catal. Calgary* **1988**, *4*, 1750–1757.
(24) Bonneviot, L.; Clause, O.; Che, M.; Manceau, A.; Dexpert, H. *Catal. Today* **1989**, *6*, 39–46.
(25) Clause, O.; Bonneviot, L.; Che, M.; Dexpert, H. Proc. 2nd European Conference on Progress in X-ray Synchrotron Radiation Reasearch; Balerna, A., Bernieri, E., Mobilio, S., Eds.; SIP: Bologna, 1990; pp 559–562.
(26) Clause, O.; Bonneviot, L.; Che, M.; Dexpert, H. *J. Catal.* **1991**, *130*, 21–28.
(27) Anderson, J. H. *J. Catal.* **1972**, *26*, 277–285.
(28) Hathaway, B. J.; Lewis, C. E. *J. Chem. Soc. (A)* **1969**, 1176–1182.
(29) Burwell, R. L., Jr.; Pearson, R. G.; Haller, G. L.; Tjok, P. B.; Chok, S. *Inorg. Chem.* **1965**, *4*, 1123–1128.
(30) Bonneviot, L.; Legendre, O.; Kermarec, M.; Olivier, O.; Che, M. *J. Colloid Interface Sci.* **1990**, *134*, 534–547.
(31) Mile, E.; Stirling, D.; Zammitt, M. A.; Lovell, A.; Webb, M. *J. Catal.* **1988**, *114*, 217–229.
(32) Mendioroz Echeverria, S.; Munoz Andres, V. *Appl. Catal.* **1990**, *66*, 73–90.

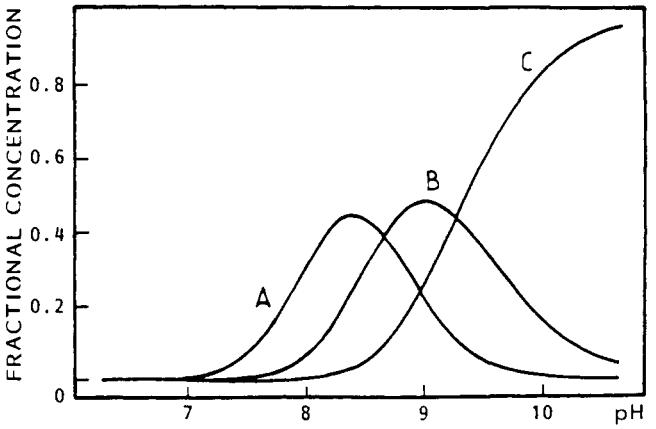

Figure 1. Amminenickel(II) complex distribution for a total Ni(II) concentration equal to 0.1 M and (NH_4^+) = 1 M; A: tetraammine Ni(II) complex; B: pentaammine Ni(II) complex; C: hexaammine Ni(II) complex.

current 300 mA). The spectra were recorded in transmission mode at ambient temperature using two air filled ionization chambers. The energy was scanned with 2- and 0.5-eV steps for EXAFS and XANES analysis, respectively, starting from 100 eV below the Ni K absorption edge. A channel-cut single crystal of silicon was used as the monochromator, the (331) reflexion being used. The XANES spectra of a thin foil of nickel was recorded before each XANES measurement to ensure a correct calibration of the energies scale. EXAFS measurements were carried out at least three times for each sample. The sample thicknesses x were chosen such that the edge jump heights (μx variation through the edge, μ being the linear absorption coefficient) ranged between 0.5 and 1.0, except for sample B (see text below), for which the μx variation was 0.2 only. In this case, however, no attempt was made to determine the second coordination shell composition, since a simple qualitative examination of the spectra was sufficient to provide relevant information. The analysis of the EXAFS spectra was performed following standard procedures for background removal, extraction of the EXAFS signal, and normalization to the edge absorption. Fourier transforms were obtained after multiplication of the EXAFS signal by a factor k^3, using the same Hanning window for the references and the investigated systems. Each shell of the radial distribution (in particular the second one, corresponding to the next nearest-backscatterer contribution) was Fourier filtered and analyzed separately.

Infrared Characterization. The samples 2%E9.8 and 3.5%Iy (with y = 5.7, 6.9, 8.3, and 9.9) were finely ground and dispersed in KBr pellets; the sample 2.7%E10.4 was conditioned as a self-supported disk. Infrared spectra were recorded on a FTIR M-1700 Perkin-Elmer spectrophotometer equipped with a 3600 data station. The resolution was 4 cm^{-1}.

Results

Ni/SiO_2 Precursors Prepared by Ion Exchange. (a) Adsorption versus pH. The adsorption of the amminenickel(II) complexes onto silica has been studied as a function of pH, the other parameters being kept constant. The composition of the exchange solutions can be described as follows: the concentrations of the $[Ni(NH_3)_n(H_2O)_{6-n}]^{2+}$ complexes with $n > 3$ and of the hydrolyzed species $[Ni(OH)]^+$, $Ni(OH)_2$, $[Ni_2(OH)_3]^+$, $[Ni_4(OH)_4]^{4+}$ have been calculated for a total concentration of Ni(II) equal to 0.1 M as a function of pH, keeping in mind that the (NH_4NO_3) concentration is 1 M in the exchange solutions. The thermodynamic equilibrium constants have been taken from ref 33. The amminenickel(II) complexes distribution is presented in Figure 1. The hexaammine complex is the main species above pH 9.5, while below pH 8 its concentration is negligible. The concentration of the tetraammine complex, which has been suggested to play a particular role in the grafting process,[30] is maximal around pH 8 and becomes negligible above pH 9.5. The hydrolyzed Ni(II) species concentrations are presented in Figure 2. All concentrations are lower than 10^{-6} M. The maximal concentration of $Ni(OH)_2$, 5.3×10^{-8} M, reached around pH 7.4, is more than 100 times smaller than the precipitation value (1.3×10^{-6} M),

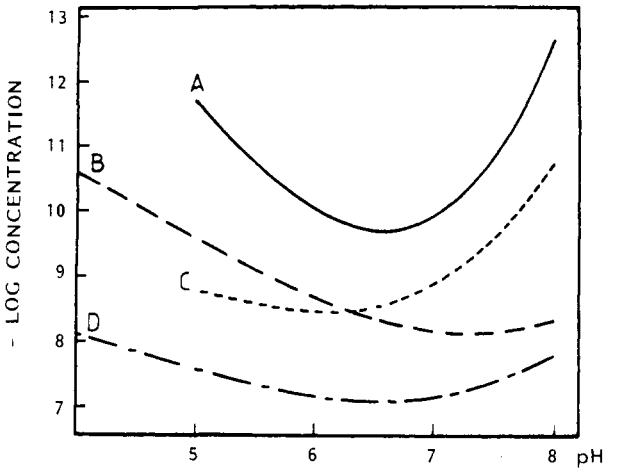

Figure 2. Distribution of the Ni(II) hydrolyzed species $[Ni_4(OH)_4]^{4+}$ (curve A), $Ni(OH)_2$ (curve B), $[Ni_2(OH)_3]^+$ (curve C), and $[Ni(OH)]^+$ (curve D), as a function of pH for a total Ni(II) concentration equal to 0.1 M and for (NH_4^+) = 1 M.

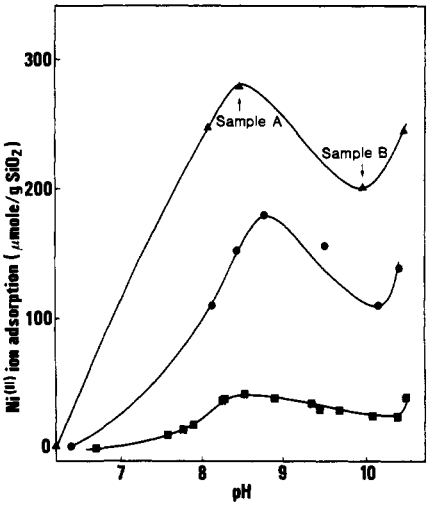

Figure 3. Adsorption of Ni(II) ions on silica at thermodynamical equilibrium as a function of pH for 0.01 (■), 0.05 (●), and 0.1 M (▲) Ni(II) initial concentrations.

so that nickel(II) hydroxide does not precipitate in the exchange solutions in the whole range pH 2–11. The silica surface being negatively charged in basic medium,[34] the local concentrations in the vicinity of the silica surface are multiplied by the Boltzmann factor $\exp(-ZeV/kT)$, where Z is the charge of the cation and V (negative) the local electric potential. However, the distribution of the amminenickel(II) complexes (all 2+ charged) remains unchanged, as well as the nickel hydroxide concentration (uncharged species).

The results concerning the adsorption of amminenickel(II) complexes at the thermodynamic equilibrium for initial Ni(II) concentrations equal to 0.01, 0.05, and 0.1 M in the exchange solutions are reported on Figure 3. The adsorption, which is very weak below pH 6.5, passes through a maximum around pH 8.6, then decreases, producing a minimum around pH 10.2, and finally increases very fast above pH 10.5.

(b) EXAFS and XANES Analysis. Choice of Convenient References. Amplitude and phase functions for the Ni···O, Ni···Ni, and Ni···Si systems were extracted from the spectra of reference compounds. Stoechiometric NiO was used as a reference for the Ni···O system. Well-crystallized $Ni(OH)_2$ was used as a reference for the Ni···Ni system. $Ni(OH)_2$ was precipitated by adding a nickel(II) nitrate solution to a sodium bicarbonate solution; the precipitate was then hydrothermally treated (250 °C, 30 amt, 50 h), and X-ray diffraction showed that the final

(33) Kragten, J. *Atlas of metal–ligand equilibria in aqueous solution*; Masson: Paris, 1978; pp 508–509.

(34) Brunelle, J. P. *Pure. Appl. Chem.* **1978**, *50*, 1211–1229.

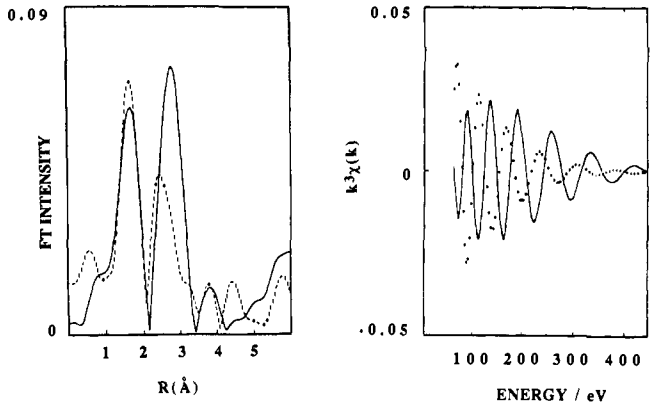

Figure 4. (a, Left) Fourier transform of the EXAFS spectra of the reference compounds $Ni(OH)_2$ (full lines) and $Mg(OH)_2$:Ni (dashed lines). (b, Right) Inverse Fourier transform of the second peaks of (a), corresponding to six Ni at 3.14 Å (full lines) and six Si at 3.14 Å (dashed lines).

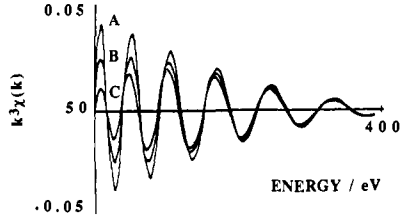

Figure 5. Inverse Fourier transform of the next-nearest-neighbor peaks of the nickel hydroxide (curve A), the nepouite (curve B), and the nickel talc (curve C).

product was well-crystallized $Ni(OH)_2$.

A Ni-doped magnesium hydroxide was used as a reference for the Ni···Si system, taking into account that $Mg(OH)_2$ and $Ni(OH)_2$ are completely miscible and that Mg and Si with very close masses can be considered as equivalent in EXAFS. The EXAFS spectra after Fourier transform of the $Ni(OH)_2$ and $Mg(OH)_2$:Ni references are presented in Figure 4a. The EXAFS spectra extracted from these references and corresponding to six Ni (reference $Ni(OH)_2$) or six Si (reference $Mg(OH)_2$:Ni) backscatterers both at 3.14 Å are presented in Figure 4b. A rapid examination of Figure 4b shows that when both Ni and Si backscatterers are present the contribution of the Ni neighbors dominates for high photoelectron energies, whereas that of Si neighbors dominates for low photoelectron energies. However, it is not obvious that $Mg(OH)_2$:Ni is a good reference for the Ni···Si system if nickel silicates are present in the samples, since Mg(II) ions in the reference and Si(IV) ions in the silicates have different valence and bonding states.[35] Therefore, we have checked the Ni···Ni and Ni···Si references by determining with the EXAFS technique the structure of two synthesized nickel silicates with layer structure, a nepouite $Ni_3(OH)_4Si_2O_5$ and a talc $Ni_3(OH)_2(Si_2O_5)_2$.[36] Furthermore, it was necessary to ensure that the EXAFS technique could distinguish a nickel(II) silicate of nepouite structure from nickel hydroxide or nickel talc. The Fourier back-transforms of the next-nearest-neighbor peaks of the nickel hydroxide, the nepouite, and the Ni talc are presented in Figure 5. The influence of silicon backscatterers is evident for low photoelectron energies. The best fits obtained for the nepouite and the nickel talc with the references mentioned above are presented in Table I. The agreement with the known structure of the silicates is correct,[36] even though the Ni···Si distances may be overevaluated because of slightly different phase functions for Mg and Si backscatterers. Thus, the references chosen for the Ni···Ni and Ni···Si systems may be considered as well adapted to our Ni/SiO_2 materials study. The Debye–Waller factors found for Ni and Si backscatterers in synthesized silicates (Table I) will be used as references for fitting EXAFS spectra of samples containing silicates.[26]

Table I. Structural Parameters for Ni/SiO_2 Samples Determined by the EXAFS Technique[a]

sample	shell atom	distance, Å	coord. no.	σ, Å	Q^*
		Model Compounds			
nepouite	Ni	3.09	6.0	0.091	0.0016
	Si	3.27	2.4	0.065	
Ni talc	Ni	3.05	6.0	0.092	0.0044
	Si	3.27	5.0	0.060	
		Nondried Silica Samples after Ion Exchange Depending on pH of the Impregnating Solution			
sample A	Ni	3.11	5.3	0.095	0.0016
	Si	3.31	2.4	0.065	
sample B		neither Ni nor Si backscatterers			
		Ni/SiO_2 Precursors Prepared by Ion Exchange after Drying			
4.3%E10.8	Ni	3.10	5.9	0.098	0.0079
	Si	3.28	3.1	0.070	
3.8%E8.3	Ni	3.10	5.9	0.098	0.0012
	Si	3.25	3.0	0.070	
2.0%E9.8	Ni	3.10	6.3	0.094	0.0084
	Si	3.24	2.3	0.070	
		Ni/SiO_2 Precursors Prepared by Incipient Wetness Impregnation as a Function of pH of Impregnating Solutions			
1.4%I5.7	O	2.07	6.1	0.0019	
		neither Ni nor Si backscatterers			
1.4%I6.9	Ni	3.12	2.4	0.101	0.0020
	Si	3.22	1.3	0.071	
1.4%I8.3	Ni	3.10	6.4	0.093	0.0195
	Si	3.30	2.0	0.071	
1.4%I9.8	Ni	3.14	2.4	0.102	0.0025
	Si	3.29	0.8	0.072	
1.4%I10.3	Ni	3.11	3.2	0.102	0.0028
	Si	3.29	1.2	0.071	
3.5%I5.7		neither Ni nor Si backscatterers			
3.5%I6.9	Ni	3.10	4.7	0.100	0.0045
	Si	3.25	2.3	0.080	
3.5%I8.5	Ni	3.09	5.7	0.095	0.0038
	Si	3.29	3.5	0.071	
3.5%I9.9	Ni	3.10	4.0	0.098	0.0071
	Si	3.24	1.8	0.071	

[a] The best fits are obtained minimizing the agreement factor Q^*. The mean free path parameter is taken equal for all references and samples. The precision on the Ni and Si backscatterer numbers is ±0.8. The precision on the distances is ±0.05 Å.

Characterization of the Ni-Containing Silica Samples after Ion Exchange and before Drying. The content of Ni(II) ions in the Ni/SiO_2 samples does not increase continuously when the pH of the impregnating solution departs from the isoelectric point of the silica (around pH 2),[34] which indicates complex adsorption phenomena. Therefore the EXAFS technique was used to investigate the different adsorption modes of Ni(II) ions onto silica for the samples corresponding to the extrema of the adsorption curve (represented by shafts in Figure 3). The samples obtained after exchange were washed with solutions containing 1 M NH_4NO_3 and at the pH of the supernatant solutions after exchange, so as to prevent the decomposition of the nickel complexes or the precipitation of $Ni(OH)_2$. Sample A (Figure 3) was obtained after exchange at pH 8.3 followed by washing until the washing solution was clear. Hence the nickel(II) species investigated by EXAFS technique are adsorbed and not located in the solution held in the pores of silica. Sample B was obtained after exchange at pH 9.8. Since it was found that a prolonged washing could remove all the adsorbed nickel, the washing step was performed so as to yield the lowest content compatible with an analysis in transmission mode. Samples A and B are samples 3.8%E8.3 and 2.0%E9.8, respectively, before drying.

The Fourier transforms of the EXAFS spectra of samples A and B (without phase correction) are given in Figure 6. The first

(35) Crozier, E. D.; Rehr, J. J.; Ingalls, R. In *X-ray Absorption: Principles, Applications, Techniques of EXAFS, SEXAFS and XANES*; Koningsberger, D. C., Prins, R., Eds.; Wiley: New York, 1988; pp 421–422.
(36) Wells, A. F. *Structural Inorganic Chemistry*; Clarendon Press: Oxford, 1984; pp 1024–1032.

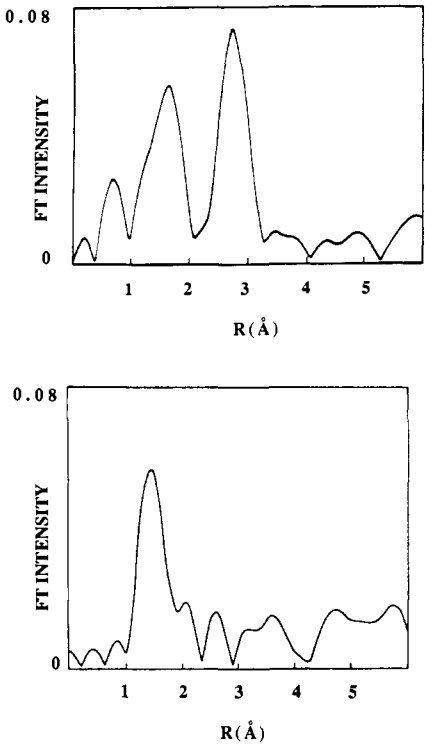

Figure 6. (a, Top) Fourier transform of the EXAFS spectrum of a Ni/SiO_2 material after ion exchange at pH 8.3 and before drying. (b, Bottom) Fourier transform of the EXAFS spectrum of a Ni/SiO_2 sample after ion exchange at pH 9.8 and before drying.

peaks characterize the first coordination shell and refer to oxygen or nitrogen atoms belonging to water or ammonia ligands. The number of first neighbors is always close to six, suggesting that Ni(II) ions keep their octahedral environment whatever of the adsorption pH. The second peaks characterize the second coordination shell and refer to oxygen, nitrogen, silicon, or nickel atoms. We observe that the second coordination shell compositions of adsorbed Ni(II) ions when exchanged onto silica at pH 8.3 (sample A) or 9.8 (sample B) are quite different. For sample B exchanged at pH 9.8, there are neither Ni nor Si next nearest neighbors, suggesting that adsorbed Ni(II) ions remain isolated and that the interaction with the surface is weak. By contrast, for sample A exchanged at pH 8.3, Ni and Si next nearest neighbors are simultaneously observed. The best fit using the reference samples is reported in Table I. Care has been taken to derive the number of such neighbors consistent with acceptable Debye–Waller factors values: the number of Ni and Si backscatterers and the corresponding Ni··Ni and Ni··Si distances are very close to those of nepouite (Table I). Thus the EXAFS technique indicates that the ion exchange of Ni(II) ions on silica leads to quite different adsorption types depending on the pH of the ammonia solutions. At pH around 10, the adsorption is weak but its exact nature cannot be determined from EXAFS measurements only. At pH around 8.3, the ion exchange leads to the formation of nickel silicates with layer structure during the impregnation step.

Effect of Drying. Figure 7 gives the Fourier back-transforms of the next-nearest-neighbor peaks for dried Ni/SiO_2 precursors obtained by ion exchange from a 0.1 M $Ni(NO_3)_2$ ammonia solution at pH 8.3, 9.8, and 10.8 (samples 3.8%E8.3, 2.0%E9.8, and 4.3%E10.8, respectively). We observe that the spectra are very similar. The compositions of the second coordination shells are reported in Table I. It can be seen that, after drying, silicates with layer structure are detected whatever the nickel loading, the composition, and the pH of the exchange solutions. As seen above for the gels exchanged at pH 8.3, nickel silicates were already formed during the impregnation step. The drying step seems to lead to an increase of the coherency domains with a number of Ni next nearest neighbors rising from 5.3 to 5.9. By contrast,

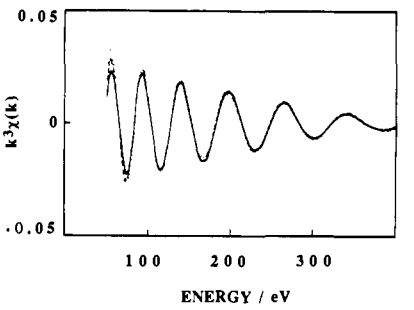

Figure 7. Inverse Fourier transform of the next-nearest-backscatterer peaks of dried Ni/SiO_2 precursors after ion exchange at pH 8.3, 9.8, and 10.8.

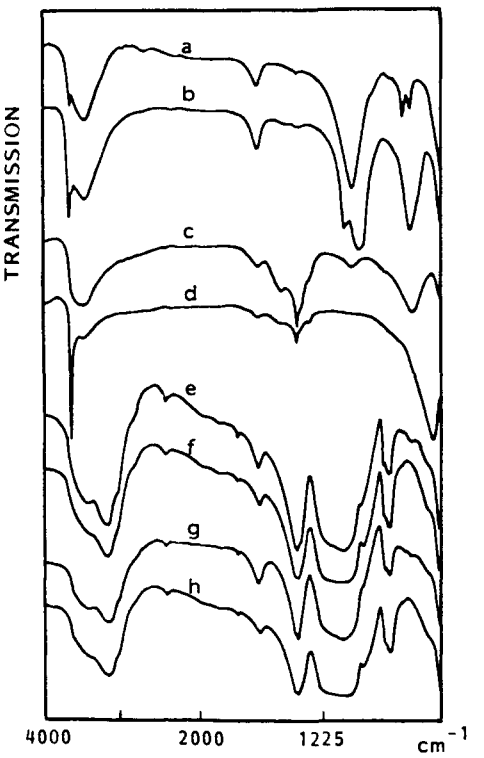

Figure 8. Infrared spectra of references samples and of two Ni/SiO_2 precursors prepared by ion exchange and incipient wetness impregnation: (a) Ni Talc synthetized at 150 °C; (b) Ni nepouite synthetized at 150 °C; (c) poorly crystallized nickel hydroxide; (d) well-crystallized nickel hydroxide; (e) 3.5%I8.3 sample; (f) Spherosil XOA400 impregnated with NH_4NO_3 at pH 8.3; (g) 2%E9.8 sample; (h) Spherosil XOA400 impregnated with NH_4NO_3 at pH 9.8.

for the gel exchanged at pH 9.8, nickel silicates are formed during drying, underlining the importance of this preparation step. The variation of the number of silicon backscatterers with Ni loading might be interpreted by the presence of a mixture of silicates of different structure. However, the low precision on the silicon backscatterers number (±0.8) does not allow evaluation accurately of a talc/nepouite ratio.

(c) Characterization by Infrared Spectroscopy. Reference Samples. Figure 8 (spectra a–d) gives the spectra of the reference samples in the 4000–450-cm^{-1} range: two Ni-layered silicate structures (talc and nepouite) synthesized at 150 °C, a poorly crystallized nickel hydroxide prepared by adding NH_3 to a solution of $Ni(NO_3)_2$, and a well-crystallized $Ni(OH)_2$ synthesized hydrothermally (this sample is also used as a reference in the EXAFS study; see the section above).

The layered silicate structures present, besides the SiO_4 vibrations around 1030 cm^{-1}, bands characteristic of structural OH groups.[37] Ni talc shows a characteristic doublet at 710–670 cm^{-1},

(37) Farmer, V. C. In *The Infrared Spectra of Minerals*; V. C. Farmer: London, pp 344.

Table II. Main Infrared Absorption Bands and Assignments

compound	wavenumber, cm^{-1}	type	assignment	group
Spherosil XOA400 impregnated in NH_4NO_3	1100	ν_{as}	SiO as stretch	SiO_4[44] in tectosilicates
	980	ν_s	SiO stretch of SiOH groups	
	800	ν_s	SiO sym stretch	
	470	δ	SiO bend	
	3150	$\nu_3(F_2)$		NH_4^+[48]
	3040	$\nu_1(A_1)$		
	1400	$\nu_4(F_2)$		
	1386	$\nu_3(E')$	NO_2 stretch	NO_3^-[49]
	827	$\nu_2(A_2'')$	out of plane	
	726	$\nu_4(E')$	NO_2 bend	
Ni talc	1030	$\nu_1(A_1)$	SiO as stretch	SiO_4[37] in TOT layer silicates
		$\nu_3(E_1)$	SiO as stretch	
	670	$\nu_2(A_1)$		
	3625	ν_{OH}	stretch	OH[39]
	710	δ_{OH}	bend	
	1069	$\nu_1(A_1)$	SiO as stretch	SiO_4[37] in TO layer silicates
	1051	$\nu_4(A_1)$	SiO as stretch	
	985	$\nu_3(E_1)$	SiO as stretch	
nepouite	670	$\nu_2(A_1)$		
		δ_{OH}	bend	OH
	3645	ν_{OH}	stretch	
well-crystallized $Ni(OH)_2$	3650	ν_{OH}	stretch	OH[42]
	520	δ_{OH}	bend	

while nepouite exhibits a single and broader band around 670 cm^- (spectra a, b). Earlier work on natural and synthetic layer silicates indicates that the 710-cm^{-1} band is due to a δ_{OH} vibration in a Ni environment. The 670-cm^{-1} band corresponds to a tetrahedral mode $\nu_2(A_1)$.[38-40] The stretching vibrations ν_{OH} are observed at 3625 and 3645 cm^{-1} for Ni talc and nepouite, respectively.

Well-crystallized $Ni(OH)_2$ is characterized by the presence of a sharp ν_{OH} stretching band at 3650 cm^{-1} and a large and broad δ_{OH} band at 520 cm^{-1}. For the poorly crystallized sample the δ_{OH} vibration is shifted toward higher frequencies (654 cm^{-1}) while ν_{OH} is not observed (spectra c, d). This behavior is explained by the presence of H_2O molecules located between disoriented layers (turbostratic compound) and in strong hydrogen bonding with the structural OH groups.[41-43]

It appears therefore that the presence of a talc-like structure in the Ni/SiO_2 precursors can be detected by the observation of two bands in the 720–670-cm^{-1} range. By contrast, when a single band is observed, it is difficult from IR spectroscopy to discriminate a silicate of nepouite-like structure from an ill-crystallized nickel hydroxide, although the position of the δ_{OH} band is slightly different in both compounds. The observation of ν_{OH} bands in the Ni/SiO_2 samples requires a calcination pretreatment in order to eliminate adsorbed ammonium and water molecules. Such a pretreatment would modify the ion-support interaction as shown below by EXAFS technique and thus must be avoided. In the following, infrared characterization will deal only with the 600–750-cm^{-1} range, which brings information on silicate formation.

Ni/SiO_2 Precursors. Figure 8 (spectra e–h) gives the spectra of Ni/SiO_2 precursors (e, g) and of the silica reference samples (f, h). The silica was washed with 1 M NH_4NO_3 solutions at the same pH as that used for the corresponding exchange and impregnation preparations. In the 1300–450-cm^{-1} range, the internal vibrations characteristic of the SiO_4 tetrahedron are observed.[44-46] The strongest band in the 1250–900-cm^{-1} range corresponds to an asymmetric vibration ←OSiO→←O, the medium band at 800 cm^{-1} characterizes the symmetric ←OSiO→ vibration, and the 470-cm^{-1} band is assigned to the bending SiO mode. The 980-cm^{-1} shoulder is assigned to a SiO stretching vibration of a silanol group.[47] Besides those vibrations, since the samples have been washed in NH_4NO_3 medium, they also show the vibrations corresponding to NH_4^+[48] and to NO_3^-.[49] All the reference and Ni/SiO_2 samples exhibit a broad NH stretching vibration in the 3040–3150-cm^{-1} range and also the main nitrate bands at 1386 and 827 cm^{-1}. Table II gathers the positions of the main IR bands and their assignments for the reference samples and the Ni/SiO_2 precursors.

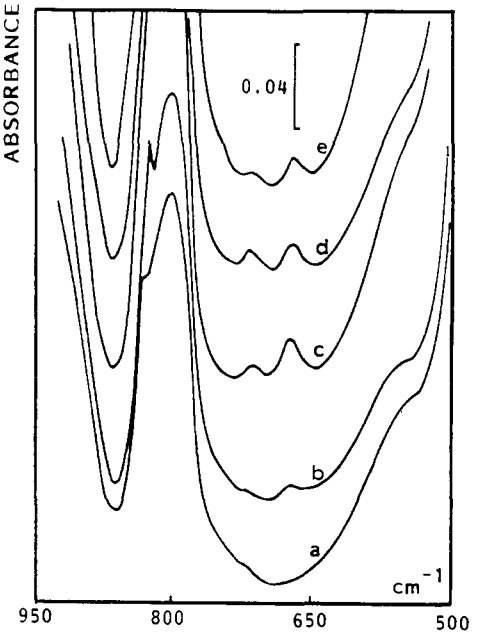

Figure 9. Infrared spectra of Ni/SiO_2 precursors prepared by ion exchange: (a) Spherosil XOA400 impregnated with NH_4NO_3 at pH 9.8; (b) 2%E9.8 sample, spectrum of the gel partially dried during KBr pelletization; (c) sample b slowly dried at 25 °C (2 months) before pelletization; (d) sample b dried at 70 °C for 48 h; (e) 2.7%E10.3 sample, self-supported disk.

Figure 9 displays the spectra of sample 2%E9.8 versus drying conditions. The spectral domain is limited to the 1100–500-cm^{-1} range, where bands characteristic of a silicate-like phase (if any)

(38) Wilkins, R. W. T.; Ito, I. *Am. Mineral.* **1967**, *52*, 1649–1661.
(39) Gérard, P.; Herbillon, A. J. *Clays Clay Miner.* **1983**, *31* (2), 143–151.
(40) Russel, J. D.; Farmer, V. C.; Velde, B. *Miner. Mag.* **1980**, *37*, 870–879.
(41) Figlarz, M.; Le Bihan, S. *C. R. Acad. Sci. Paris* **1971**, *272*, 580–583.
(42) Le Bihan, S.; Figlarz, M. *J. Cryst. Growth* **1972**, *13*, 458–461.
(43) Le Bihan, S.; Figlarz, M. *Thermochim. Acta* **1973**, *6*, 319–326.
(44) Lippincot, E. R.; Van Valkenberg, A.; Weir, C. E.; Bunting, E. N. *J. Res. Natl. Bur. Stand.* **1958**, *A 61*, 61–70.
(45) Lazarev, A. N. *Vibrational Spectra and Structure of Silicates*; Plenum Press: New York, 1972.
(46) Flanigen, E. M.; Khatami, H.; Szymanski, H. A. *Adv. Chem. Ser.* **1971**, *101*, 201–229.
(47) Hino, M.; Sato, T. *Bull. Chem. Soc. Jpn.* **1971**, *44*, 33–37.
(48) Nakamoto, K. *Infrared and Raman Spectra of Inorganic and Coordination Compounds*; Wiley: New York, 1978; p 135.
(49) Addison, C. C.; Gatehouse, B. M. *J. Chem. Soc.* **1960**, 613–615.

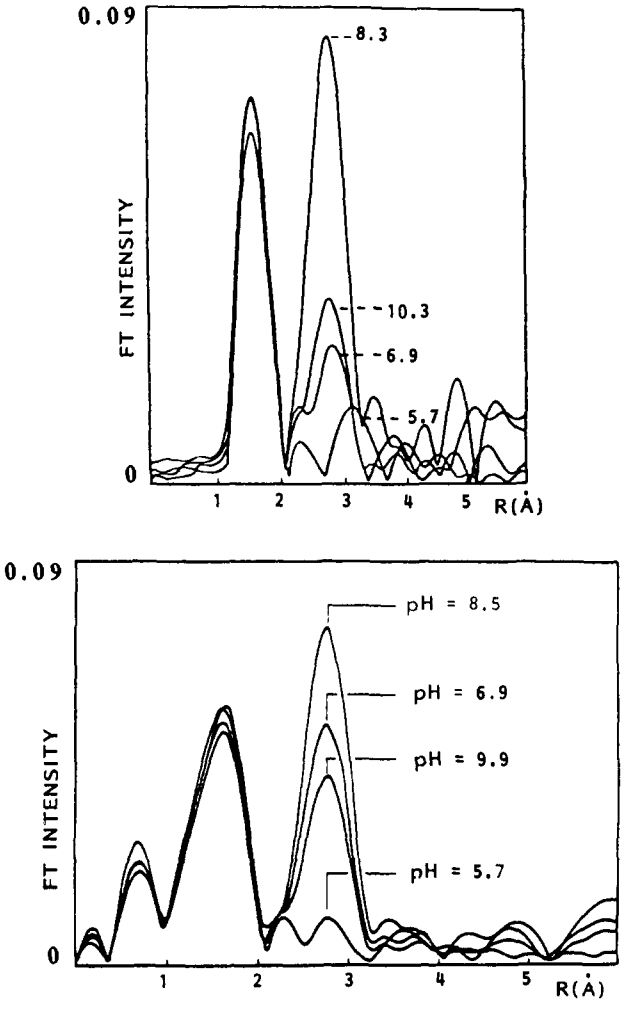

Figure 10. Fourier transform of the EXAFS spectra of two sets of dried Ni/SiO_2 precursors after incipient wetness impregnation by solutions at pH 5.7, 6.9, 8.3, and 10.3. (a, Top) Ni loading: 1.4 wt %. (b, bottom) Ni loading: 3.5 wt %.

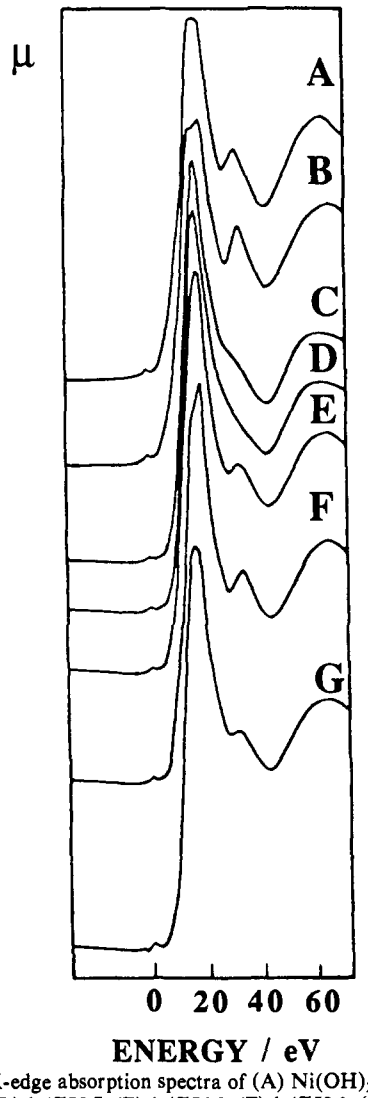

Figure 11. Ni K-edge absorption spectra of (A) $Ni(OH)_2$; (B) Ni talc; (C) $Ni(NO_3)_2$; (D) 1.4%I5.7; (E) 1.4%I6.9; (F) 1.4%I8.3; (G) 1.4%I10.3.

can be detected between the two bands of silica at 800 and 470 cm^{-1}.

It was not possible to obtain the spectrum of the blue magenta gel corresponding to the hexaammine complex, since mixing the gel with KBr partly removed NH_3 with the sample turning green. The spectrum of this sample obtained after a short time of drying at 25 °C shows, besides the symmetric stretching band of silica at 800 cm^{-1}, very weak bands around 710 and 670 cm^{-1} (spectrum b). After staying in air at 25 °C for 2 months, the sample exhibits the doublet at 710–670 cm^{-1} characteristic of a talc-like structure (spectrum c). Drying at 70 °C for 48 h leads to an increase of the intensity of the 716-cm^{-1} band at the expense of the 670-cm^{-1} one.

The observation of the 710-cm^{-1} band in the Ni/SiO_2 precursors indicates the presence of a talc-like phase. However in Ni talc the latter band is slightly more intense than the 670-cm^{-1} band (Figure 8a). The reverse situation in our precursors may indicate that another phase is present. This phase may be identified to nepouite or $Ni(OH)_2$, although the δ_{OH} band of an ill-crystallized hydroxide sample appears at a lower frequency (654 cm^{-1}) than the δ_{OH} band of nepouite (670 cm^{-1}). The formation of a poorly crystallized talc-like phase also accounts for the weaker intensity of the δ_{OH} band.[50]

Ni/SiO_2 Precursors Prepared by Incipient Wetness Impregnation. (a) Influence of pH. EXAFS and XANES Analysis. The EXAFS spectra after Fourier transform of Ni/SiO_2 precursors prepared by incipient wetness impregnation are presented in Figure 10 as a function of the pH of the impregnating solutions. The first coordination shells are very similar and their compositions may be easily obtained with oxygen backscatterers only. A typical fit is given in Table I. The fits for the other samples, being identical, have been omitted. The result of the first coordination shell analysis is that Ni(II) ions keep their octahedral environment whatever the composition of the impregnating solutions.

An examination of Figure 10 shows that the next-nearest-neighbor peaks of Ni(II) ions strongly depend on the pH of the impregnating solutions. The fits are gathered in Table I. When the pH of the impregnating solutions is acidic (for instance pH 5.7) there are neither Ni nor Si backscatterers in the second coordination shell and the spectra are similar to that of nickel nitrate. When the pH increases, peaks due to Ni and Si backscatterers appear simultaneously. For the sample prepared at pH 8.3, all Ni(II) ions are involved in silicates. In the other samples, the Ni and Si backscatterer numbers N_{Ni} and N_{Si} are lower than those of their analogues in silicates, but the value of the ratio N_{Ni}/N_{Si} remains between 2 and 3. Hence the mathematical fitting of the EXAFS spectra is consistent with the following description of the Ni/SiO_2 precursors: a part of Ni(II) ions react with silica to form nickel silicates, the other part recrystallizing in the pores of silica as nickel(II) nitrate (in the latter, there is no Ni contribution to the second coordination shell). The fraction of silicates formed as a function of the pH of the impregnating solutions may be estimated as the ratio of the value of N_{Ni} in the investigated samples to that in Ni talc or nepouite ($N_{Ni} = 6$).

The importance of the pH of the impregnating solutions is confirmed by XANES measurements. The K absorption edges

(50) Decarreau, A., private communication.

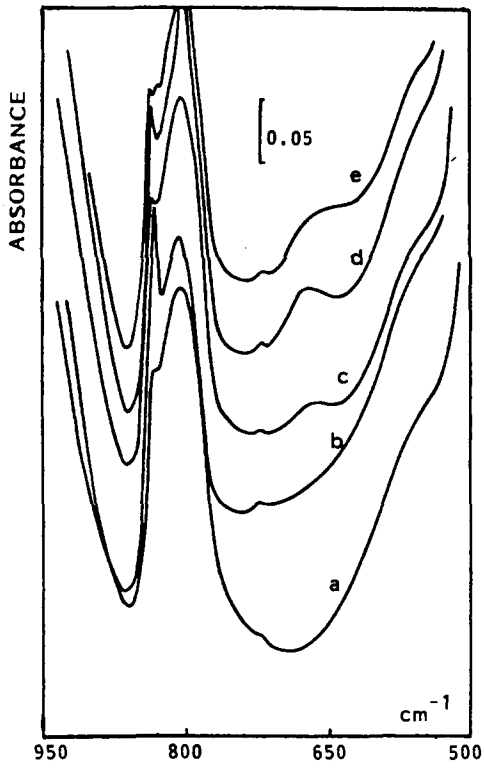

Figure 12. Infrared spectra of Ni/SiO_2 precursors prepared by incipient wetness impregnation at various pHs: (a) XOA 400 impregnated with NH_4NO_3 at pH 8.3; (b) 3.5%I5.7 sample; (c) 3.5%I6.9 sample; (d) 3.5%I9.8 sample; (e) 3.5%I8.3 sample.

of nickel in $Ni(OH)_2$, Ni talc, and $Ni(NO_3)_2$ precursors are displayed in Figure 11. All spectra present a strong absorption at 8345 eV characteristic of octahedrally coordinated Ni(II) ions. A splitting of the main edge structure, likely due to a distorsion of Ni(II) octahedral symmetry, is observed in the nickel talc and the nickel hydroxide spectra. Tetrahedrally coordinated Ni(II) ions, characterized by a shoulder in the absorption slope,[51] are not present in detectable amount in the references or in the Ni/SiO_2 samples. Although the symmetry of Ni(II)-deposited ions remains octahedral, spectra D–G present some differences related to the pH of the impregnating solutions. When pH 8.3, the spectrum exhibits a peak or a shoulder around 35 eV above the edge (Figure 11F). This peak is attenuated for pH 10.3 and is absent for pH 5.7. This feature is also present in the spectra of Ni talc and nickel hydroxide, whereas it is absent in the spectrum of nickel nitrate. A peak at the same position is present in the spectra of the samples prepared with solutions at pH 6.9, 8.3, and 10.3 (Figure 11E,F,G, respectively). Its intensity reaches a maximum for pH 8.3. This observation is well accounted for by the distribution of Ni(II) ions both as nickel silicates and nickel nitrate crystallized in the pores of the carrier. The nickel nitrate concentration dependence on pH of the impregnating solutions is qualitatively that shown by the EXAFS analysis in the previous paragraph; i.e., no nitrates are formed at pH 8.3, while only nitrates are formed at acidic pH (see Table I also). However, it is not possible from XANES spectroscopy to distinguish whether Ni(II) ions form silicates or nickel hydroxide epitaxially "glued" onto silicate layers.

(b) Influence of pH. Infrared Characterization. All samples have been dried directly after the impregnation process without any subsequent washing. Thus they contain ammonium nitrate crystallized in the pores of silica giving rise to the main nitrate vibrations at 1386 and 827 cm^{-1} (Figure 8e and Table II).

The spectra of samples prepared at various pHs are depicted in Figure 12. For pH above 6.9 (spectra c–e) a broad band around 670 cm^{-1} is observed together with a very weak peak at about 720 cm^{-1}. The latter peak is also present in the spectra of silica XOA 400 impregnated with a NH_4NO_3 1 M solution at pH = 8.3 (spectrum a). It may be assigned to the vibration of NO_3^- ion, always very weak, rather than to the δ_{OH} band of a talc-like structure. The 670-cm^{-1} band increases in intensity to reach a maximum for pH 8.3 (spectrum d) but is absent for sample 3.5%I5.7 (spectrum b). The evolution of the 670-cm^{-1} band intensity as a function of the pH of the impregnating solution is very similar to that of the second coordination peak followed by the EXAFS technique (Figure 10). This result is thus consistent with the EXAFS analysis, even though infrared spectroscopy, as XANES spectroscopy, does not allow one to distinguish clearly between nickel hydroxide or nickel silicate formation.

Discussion

The impregnation of Ni(II) ions onto silica from ammonia solution leads to quite different adsorption types depending on the preparation parameters such as the pH, the composition of the impregnating solutions, and the washing and drying operations. EXAFS technique yields very useful information first on ion–surface bonding through the Si next-nearest-neighbor number and second ion–ion interaction during adsorption through the Ni next-nearest-neighbor number. On the other hand, XANES and infrared spectroscopies bring confirmation on the presence of silicates. The various types of ion–support interactions are now discussed.

1. Recrystallization of Nickel Ammine Nitrate Salts $[Ni(H_2O)_x(NH_3)_{6-x}](NO_3)_2$ in the Pores and on the Surface of Silica. The Carrier as Dispersing Agent. The recrystallization of nickel(II) salts is not observed after ion exchange and subsequent washing with distilled water, the disappearance of nitrate ions being confirmed by UV spectroscopy.[30] The presence of nitrates is evidenced only when there is no washing operation involved. The incipient wetness impregnation of Ni(II) ions onto silica only leads to nickel nitrate formation when the pH of the impregnation solutions is acidic (pH <6). When the pH exceeds 6, a mixture of $Ni(NO_3)_2$ and nickel silicates with layer structure is observed. The interaction of nickel nitrate crystallized in the pores with the support is weak since the salt is easily removed by washing with aqueous solutions. NiO is formed upon calcination at low temperatures (<400 °C).

2. Electrostatic Adsorption of $[Ni(NH_3)_6]^{2+}$ on Silica. The Carrier as Macroanion. This adsorption mode occurs during ion exchange at pH above 9.6. EXAFS results show that there is no silicon next nearest backscatterer around the adsorbed Ni(II) ions, indicating that the interaction of the latter with the surface is weak. This is confirmed by the observation that $[Ni(NH_3)_6]^{2+}$ complexes are removed by washing with ammonia solutions at pH 9.8, whereas for silica gels exchanged at pH 8.3 washing with ammonia solutions at the same pH only removes a slight fraction of the Ni(II) adsorbed ions: $\equiv SiO^-$ groups play the role of counterions without entering the nickel(II) hexaammine coordination sphere. These results are consistent with a previous UV study that showed the disappearance of nitrate ions by washing with concentrated ammonia solutions.[30] Ni(II) and Cu(II) ions can be also electrostatically adsorbed on silica after drying at ambient temperature when ethylenediamines are the ligands instead of ammonia.[23,24]

Though the EXAFS spectra of $Ni(NO_3)_2$ crystallites and electrostatically adsorbed Ni(II) on silica are indistinguishable, the interactions of those species with the support are very different. The difference is clearly illustrated by drying in an oven. In the first case, washing with water after drying removes the nickel nitrate from the carrier. In the second case, drying leads to silicate with layer structure formation involving the whole adsorbed Ni(II) fraction and the silicates will not be removed by a subsequent washing.

3. Formation of Nickel Silicates. The Carrier as "Chemical Reagent". The formation of nickel silicates with layer structure during the preparation of Ni/SiO_2 precursors appears to be highly favored whatever the preparation method, incipient wetness impregnation, ion exchange, or deposition–precipitation.[26] In the case of ion exchange from Ni(II) ammonia solutions, silicates are

(51) Niemann, W.; Clausen, B. S.; Topsoe, H. *Catal. Lett.* **1990**, *4*, 355–364.

formed as early as the impregnation step if the pH of the impregnating solution is around 8.3 (Figure 6a). For pH about 9.5 the complexation of Ni(II) to form a hexaammine complex inhibits the silicate formation. A subsequent drying, however, leads to the decomposition of the complexes, which allows the formation of silicates. A similar effect is observed after ion exchange upon washing with water instead of ammonia solutions.

The silicate formation upon drying can be inhibited by using ethylenediamine instead of ammonia as a ligand.[24] In this case, the grafting of isolated Ni(II) ions onto silica is obtained upon calcination at low temperatures (<500 °C). This behavior can be explained by the chelating character of ethylenediamine as ligand, making the "shield" around Ni(II) ions against silicate formation more effective. By contrast, this study shows that the grafting of isolated Ni(II) ions is not obtained by adsorption from amminenickel(II) solution whatever the pH of the solution.

4. Interpretation of the Ni(II) Adsorption Profiles. We may now interpret the Ni(II) adsorption profiles during ion exchange as a function of pH (Figure 3). Below pH 6, the absence of adsorption is explained by the vicinity of the isoelectric point of silica (around 2): the surface charge density is very low[34] and the amount of Ni(II) complexes adsorbed electrostatically is therefore negligible. On the other hand, the dissolution of silica is also negligible, hence nickel silicates cannot form. The EXAFS investigation shows that the adsorption increase above pH 7 is related to the silicate formation. The adsorption around pH 10 is electrostatic in nature and is quantitatively limited, the competition with NH_4^+ ions being important. Between pH 8 and 10, it is likely that the ion exchange of Ni(II) ions onto silica gives rise to a mixture of nickel silicates and Ni(II) electrostatically adsorbed. Above pH 9.5, the hexaammine Ni(II) complex prevails in solution (Figure 1). It is thus clear that the complexation of Ni(II) as hexaamminenickel(II) inhibits the silicate formation. The adsorption decrease between pH 8 and 10 is due to the increase of hexaamminenickel(II) concentration. The sharp adsorption increase when the pH exceeds 10.6 can be attributed to the dissolution of silica, which becomes important above pH 8; the mechanism proposed by Iler[52] explains how the dissolution of silica leads to a significant increase of the silanol groups density and hence of the exchange capacity of silica.

The extent to which the ion-exchange method of Ni(II) on silica achieves a true ion exchange between surface protons and Ni(II) ions is limited to the hexaamminenickel(II) adsorption. The ion exchange may be represented as

$$2{\equiv}SiOH + [Ni(NH_3)_6]^{2+} \leftrightarrow (2SiO^-)\cdots[Ni(NH_3)_6]^{2+} + 2H^+$$

or

$$2{\equiv}SiO^- NH_4^+ + [Ni(NH_3)_6]^{2+} \leftrightarrow (2SiO^-)\cdots[Ni(NH_3)_6]^{2+} + 2NH_4^+$$

EXAFS technique shows that adsorption is not accompanied by ligand displacement. However, when Ni(II) ions are not shielded as hexaamminenickel(II) complexes, the adsorption directly leads to silicate formation and this adsorption process cannot obviously be described by a simple proton or ammonium exchange as above. Furthermore, in nickel silicates the SiO_4 unit arrangement is very different from the SiO_4 arrangement in silica; hence the nickel silicate formation also involves a partial dissolution of silica. On the other hand, it is possible that Ni(II) cations undergo hydrolysis before silicate formation, as described below:

$$[Ni(H_2O)_2(NH_3)_4]^{2+} \leftrightarrow [Ni(OH)(H_2O)(NH_3)_4]^+ + H^+$$

The lack of water ligand in the hexaamminenickel(II) complexes would thus explain why silicates are not generated when $[Ni(NH_3)_6]^{2+}$ is the main species in solution.

We observe that the adsorption curves of Ni(II) ions from ammonia solutions onto silica give information on the possible existence of different adsorption processes on silica. This method may easily apply to the study of adsorption of other cations such as Cu(II), Zn(II), Co(II), and Cr(III) on silica. For example, adsorption curves presenting local maxima and minima with pH for Cu(II) and Zn(II) cations have been observed by other authors[53] and us.[23] As in the case of Ni(II) ions, there are for each cation at least two adsorption modes on silica, a weak adsorption of electrostatic nature concerning $[Cu(NH_3)_4]^{2+}$ or $[Zn(NH_3)_4]^{2+}$ and a strong adsorption for pH of impregnation solutions ranging between 7.0 and 8.5. Investigations of adsorption as a function of pH give also interesting results using carriers other than silica: the adsorption curves of Ni(II) ions as a function of pH on γ alumina present a maximum around pH 7.2, while with titania as carrier the maximum occurs around pH 7. In both cases, $[Ni(NH_3)_6]^{2+}$ electrostatically adsorbs above pH 10, and the adsorption maxima are close to the isoelectric points of the carriers. Some additional work is needed to establish if the adsorption maxima are due to the grafting of isolated ions or to the formation of surface compounds for those carriers.

Conclusions

In this work, the crucial importance of the first preparation steps of Ni/SiO_2 materials has been pointed out: first, the ion–support interaction can be monitored by varying the pH of the impregnating solution, pH acting as a complex switcher; silicates are formed when the pH is around 8.3 and hexaamminenickel(II) ions are electrostatically adsorbed when the pH is higher than 9.5. Depending on pH and on the washing step the support may act as a dispersing agent (carrier function), a macroanion, or a chemical reagent. Second, the role of the *drying step* is evidenced: the removal upon drying of ammine ligands from the coordination sphere of electrostatically adsorbed $[Ni(NH_3)_6]^{2+}$ complexes leads to silicate formation.

The nonelectrostatic nature of the adsorption (specific adsorption) of aqua complexes of various transition-metal ions has already been recognized by many authors.[54,55] Moreover, the interaction between adsorbed M^{n+} ions at the solid–liquid interface, leading to M–O(H)–M bonds, is pointed out in this study. When Ni(II) ions are adsorbed on silica at pH 8.3, silicates of nepouite or talc-like structure with such M–O(H)–M bonds are formed during impregnation. An investigation of the adsorption of amminecopper(II) complexes onto silica is in progress; as in the case of Ni(II) ion adsorption, isolated grafted ions are generated by neither ion exchange nor incipient wetness impregnation from ammonia solutions. The formation of Cu–O(H)–Cu bonds, well characterized by EXAFS technique through the Cu next-nearest-neighbor number, occurs whatever the preparation procedure. In this case, however, silicates are not formed.

The formation of polynuclear grafted species during impregnation can be readily characterized by EXAFS provided that the difference between the atomic number of the adsorbed ions and silicon is high enough to distinguish the EXAFS contribution of both elements. This condition is fulfilled for most precursors of supported metal catalysts. Thus the EXAFS investigation of the first steps of the materials preparation, using the adsorbed ions as microstructural probes, may provide interesting information not only on ion–support but also on ion–ion interactions at the liquid–solid interface.

Acknowledgment. We thank Prof. A. Decarreau (Université de Poitiers, France) for the gift of nickel silicate samples, Drs. C. Marcilly and C. Cameron (IFP, Rueil-Malmaison, France) and Dr. H. Dexpert (Lure, Orsay) for their interest and advice concerning sample preparation and characterization, and M. Varin for help in graphic design.

(52) Iler, R. K. *The Chemistry of Silica*; Wiley: New York, 1979; p 557.

(53) Fuerstenau, D. W.; Osseo-Asare, K. *J. Colloid Interface Sci.* **1987**, *118*, 524–542.

(54) Davis, J. A.; Leckie, J. O. *J. Colloid Interface Sci.* **1978**, *67*, 90–107.

(55) Hachiya, K.; Sasaki, M.; Saruta, Y.; Mikami, N.; Yasunaga, T. *J. Phys. Chem.* **1984**, *88*, 23–31.